J|A|C|S ARTICLES

Published on Web 03/25/2010

Mapping the Distribution of an Individual Chromophore Interacting with Silica-Based Nanomaterials

Boiko Cohen,[†] Felix Sanchez,[‡] and Abderrazzak Douhal*[,†]

Departamento de Química Física, Sección de Químicas, Facultad del Medio Ambiente and INAMOL, Universidad de Castilla−La Mancha, Carlos III S/N 45071 Toledo, Spain, and Instituto de Química Orgánica, CSIC, C/Juan de la Cierva, 3, E-28006, Madrid, Spain

Received January 28, 2010; E-mail: Abderrazzak.Douhal@uclm.es

Abstract: Exploring the interactions of molecules with silica-based mesoporous and nanoparticle materials at the atomic level and understanding of the forces that govern such H-bonds and electrostatic interactions are of fundamental importance to nanocatalysis, nanomedicine, and nanophotonics. In our approach, we studied in single-molecule time and spectral domains a proton-transfer chromophore complexed (by diffusion) and covalently bonded to MCM-41 mesoporous nanomaterial and silica particles. The results reveal strong dependence of the distribution and behavior of the interacting single molecule with the nanopores on the mode of sample preparation and nature of the involved interaction. The change at the single molecule level results in an up to 126 nm (∼4650 cm^{-1}) spectral shift (from 462 to 588 nm) and almost two times longer lifetime. Furthermore, a change in the electronic charges of the mesoporous framework results in significant narrowing in the emission band of the guest. The results are explained in terms of electronic nanoconfinement but at a single-molecular level.

Introduction

Silica-based mesoporous and zeolite materials represent a class of materials of particular interest due to their application in various fields of science and technology such as catalysis,[1] photonics,[2,3] and medicine.[4] In the first application, these materials are being used as catalytic microreactors, and as such, the main attention has been paid to relate their properties to the outcome of the hosted reactions. Mesoporous materials, such as MCM-41, have been proposed as drug carriers, and the unique environment provided by their nanochannels has been found to enhance the solubility of anticancer drugs, such as camptothecin.[5]

Single molecule spectroscopy (SMS) provides in-depth information on the behavior of a single chromophore probing the local environment in various biological and chemical systems.[6−14] Monitoring specific properties of a single chromophore, embedded and interacting with its local environment, can provide invaluable information for numerous important systems, such as glass-forming molecular liquids, photoconducting polymers, or porous materials.[15,16] SMS and fluorescence microscopy imaging have been applied for studying the interaction of several important anticancer drugs, such as camptothecin and doxorubicin, with MCM-41.[5,17] Recent developments in the field of SMS have made it possible to study various processes and reactions at resolutions well below the diffraction limit.[18−22] Subdiffraction resolution single-molecule techniques have been applied to study the catalytic reactions or to characterize the photocatalytic active sites, where the catalyst was either Ti-MCM-41 mesoporous silica or ZSM-22 and ZSM-5 zeolite.[23,24] Furthermore, SMS was applied to studying

[†] Universidad de Castilla-La Mancha.
[‡] Instituto de Química Orgánica.

(1) Corma, A. *J. Catal.* **2003**, *216*, 298.
(2) Ellison, E. H. *J. Phys. Chem. B* **2005**, *109*, 20424.
(3) Busby, M.; Kerschbaumer, H.; Calzaferri, G.; De Cola, L. *Adv. Mater.* **2008**, *20*, 1614.
(4) Vallet-Regi, M.; Balas, F.; Arcos, D. *Angew. Chem., Int. Ed.* **2007**, *46*, 7548.
(5) Lu, J.; Liong, M.; Zink, J. I.; Tammanoi, F. *Small* **2007**, *3*, 1341.
(6) Bolinger, J. C.; Fradkin, L.; Lee, K.-J.; Palacios, R. E.; Barbara, P. F. *Proc. Natl. Acad. Sci. U. S. A.* **2009**, *106*, 1342.
(7) Zeng, Y.; Liu, H.-W.; Landes, C. F.; Kim, Y. J.; Ma, X.; Zhu, Y.; Musier-Forsyth, K.; Barbara, P. F. *Proc. Natl. Acad. Sci. U. S. A.* **2007**, *104*, 12651.
(8) Barbara, P. F.; Gesquiere, A. J.; Park, S.-J.; Lee, Y. J. *Acc. Chem. Res.* **2005**, *38*, 602.
(9) Orrit, M.; Bernard, J. *Phys. Rev. Lett.* **1990**, *65*, 2716.
(10) Moerner, W. E.; Kador, L. *Phys. Rev. Lett.* **1989**, *62*, 2535.
(11) Vallee, R. A. L.; Marsal, P.; Braeken, E.; Habuchi, S.; De Schryver, F. C.; Van der Auweraer, M.; Beljonne, D.; Hofkens, J. *J. Am. Chem. Soc.* **2005**, *127*, 12011.
(12) Macklin, J. J.; Trautman, J. K.; Harris, T. D.; Brus, L. E. *Science (Washington, D. C.* **1996**, *272*, 255.
(13) Xie, X. S.; Dunn, R. C. *Science (Washington, DC, U. S.)* **1994**, *265*, 361.
(14) Betzig, E.; Chichester, R. J. *Science (Washington, DC, U. S.)* **1993**, *262*, 1422.
(15) Kulzer, F.; Xia, T.; Orrit, M. *Angew. Chem., Int. Ed.* **2010**, *49*, 854.
(16) Marawske, S.; Doerr, D.; Schmitz, D.; Koslowski, A.; Lu, Y.; Ritter, H.; Thiel, W.; Seidel, C. A. M.; Kuehnemuth, R. *ChemPhysChem* **2009**, *10*, 2041.
(17) Lebold, T.; Jung, C.; Michaelis, J.; Braeuchle, C. *Nano Lett.* **2009**, *9*, 2877.
(18) Hell, S. W. *Science (Washington, DC, U. S.)* **2007**, *316*, 1153.
(19) Heilemann, M.; Dedecker, P.; Hofkens, J.; Sauer, M. *Laser Photonics Rev.* **2009**, *3*, 180.
(20) Betzig, E.; Patterson, G. H.; Sougrat, R.; Lindwasser, O. W.; Olenych, S.; Bonifacino, J. S.; Davidson, M. W.; Lippincott-Schwartz, J.; Hess, H. F. *Science (Washington, DC, U. S.)* **2006**, *313*, 1642.
(21) Heilemann, M.; van de Linde, S.; Schuttpelz, M.; Kasper, R.; Seefeldt, B.; Mukherjee, A.; Tinnefeld, P.; Sauer, M. *Angew. Chem., Int. Ed.* **2008**, *47*, 6172.
(22) Dedecker, P.; Flors, C.; Hotta, J.-i.; Uji-i, H.; Hofkens, J. *Angew. Chem., Int. Ed.* **2007**, *46*, 8330.

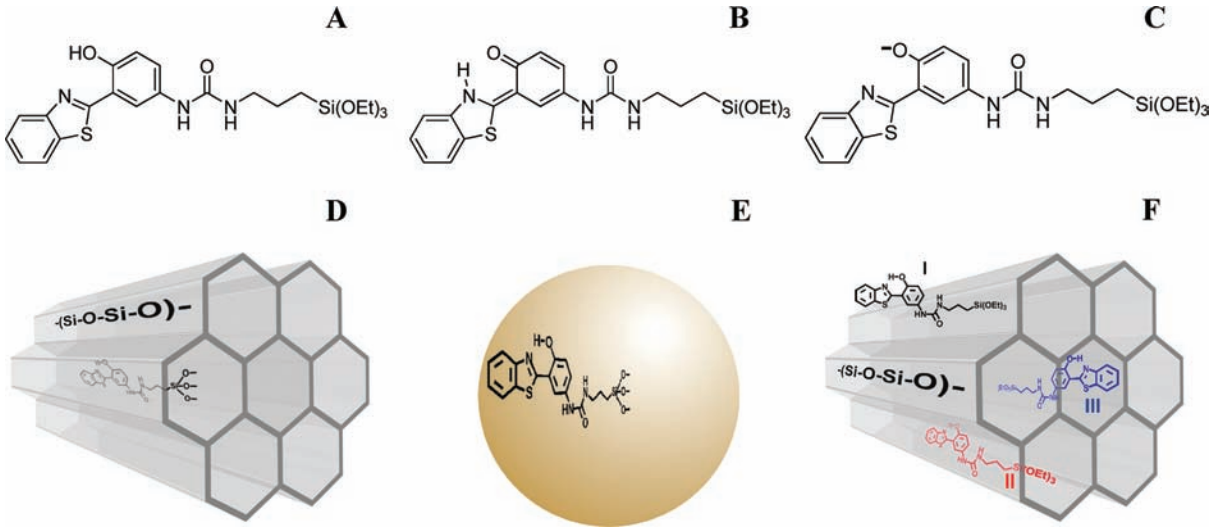

Figure 1. Molecular structure of 2-[5′-N-(3-triethoxysilyl)propylurea-2′-hydroxyphenyl]benzothiazole (HBTNH2) and schematic representation of HBTNH2−mesoporous silica material and HBTNH2− silica nanoparticle complexes: (A) enol, (B) keto, and (C) anion forms. To form the anion, the proton from the enol form (A) has been removed through an intermolecular proton-transfer process to the environment. (D) Molecular structure of 2-[5′-N-(3-triethoxysilyl)propylurea-2′-hydroxyphenyl]benzothiazole (HBTNH2) in a schematic presentation, covalently bonded inside the channel of the MCM-41 framework. (E) HBTNH2 covalently bonded to the surface of a silica nanoparticle in a schematic presentation. (F) HBTNH2 interacting with the MCM-41 framework with three possible sites of interaction: at the surface (I), inside the channel (II), and at the gate (III). For simplicity the OH groups and the nanochannels (in the case of silica nanoparticle) are omitted from the schemes. The presentations are not in scale.

and characterizing some aspects of the zeolite host−guest interactions, focusing mainly on the diffusion of a dye within its framework or on the catalytic reaction.[25−31]

Recently, we have reported on the ensemble average fast and ultrafast dynamics of Sudan I and a palladium phthalocynaine derivative caged within faujasites and MCM-41 in suspension.[32−34] The results were explained in terms of confinement effects imposed by the nanocavity or nanochannel of the host. These studies, however, revealed the complex nature of the interactions of a guest inside the nanohosts. Here we show in time-resolved and spectrally resolved domain on a single-molecule level that depending on the mode of the guest:host complex preparation different sites of the host (MCM-41) are accessed by the guest. As a result, three different populations located inside, outside, and at the gates of MCM-41, respectively, are found in the sample prepared by physical sorption of the guest. The characteristic emission change at the single-molecule level results in an up to 126 nm (∼4650 cm^{-1}) spectral shift (from 462 to 588 nm) and almost two times longer lifetime. These populations are correlated to those found in the covalently bonded single molecules within MCM-41 nanochannels and to silica nanoparticles. Remarkably, the electronic nanoconfinement of the phenolate-type anion of the guest by an Al-doped MCM-41 induces dramatic narrowing of its emission band. We selected 2-[5′-*N*-(3-triethoxysilyl)propylurea-2′-hydroxyphenyl]benzothiazole (HBTNH2, Figure 1), a derivative of 2-(2′-hydroxyphenyl)benzothiazole (HBT), whose ensemble average photodynamics is well characterized both in solution and in mesoporous silicates.[35−40] The emission spectroscopy and dynamics of 2′-hydroxyphenyl benzazol derivatives have been largely studied in the gas phase, in solution, and in polymeric matrices using a wide range of techniques.[41−44] They have been proposed as lasing media,[45,46] information storage,[47] and protectors from UV radiation,[48] in addition to local fluorescent molecular probes in organized and biological media.[43] The guest selected here, HBTNH2, shows a large Stokes-shifted emission band, which allows the detection of its fluorescence without contribution from

(23) Roeffaers, M. B. J.; De Cremer, G.; Libeert, J.; Ameloot, R.; Dedecker, P.; Bons, A.-J.; Bueckins, M.; Martens, J. A.; Sels, B. F.; De Vos, D. E.; Hofkens, J. *Angew. Chem., Int. Ed.* **2009**, *48*, 9285.
(24) De Cremer, G.; Roeffaers, M. B. J.; Bartholomeeusen, E.; Lin, K.; Dedecker, P.; Pescarmona, P. P.; Jacobs, P. A.; De Vos, D. E.; Hofkens, J.; Sels, B. F. *Angew. Chem., Int. Ed.* **2010**, *49*, 908.
(25) Zuerner, A.; Kirstein, J.; Doeblinger, M.; Braeuchle, C.; Bein, T. *Nature (London, U. K.)* **2007**, *450*, 705.
(26) Roeffaers, M. B. J.; Hofkens, J.; De Cremer, G.; De Schryver, F. C.; Jacobs, P. A.; De Vos, D. E.; Sels, B. F. *Catal. Today* **2007**, *126*, 44.
(27) Roeffaers, M. B. J.; Sels, B. F.; Uji-i, H.; De Schryver, F. C.; Jacobs, P. A.; De Vos, D. E.; Hofkens, J. *Nature (London, U. K.)* **2006**, *439*, 572.
(28) Xu, W.; Kong, J. S.; Yeh, Y.-T. E.; Chen, P. *Nat. Mater.* **2008**, *7*, 992.
(29) Kirstein, J.; Platschek, B.; Jung, C.; Brown, R.; Bein, T.; Braeuchle, C. *Nat. Mater.* **2007**, *6*, 303.
(30) Ye, F.; Collinson, M. M.; Higgins, D. A. *Phys. Chem. Chem. Phys.* **2009**, *11*, 66.
(31) Tachikawa, T.; Yamashita, S.; Majima, T. *Angew. Chem., Int. Ed.* **2010**, *49*, 432.
(32) Synak, A.; Gil, M.; Organero, J. A.; Sanchez, F.; Iglesias, M.; Douhal, A. *J. Phys. Chem. C* **2009**, *113*, 19199.
(33) Gil, M.; Organero, J. A.; Peris, E.; Garcia, H.; Douhal, A. *Chem. Phys. Lett.* **2009**, *474*, 325.
(34) Gil, M.; Wang, S.; Organero, J. A.; Teruel, L.; Garcia, H.; Douhal, A. *J. Phys. Chem. C* **2009**, *113*, 11614.
(35) Mintova, S.; De Waele, V.; Hoelzl, M.; Schmidhammer, U.; Mihailova, B.; Riedle, E.; Bein, T. *J. Phys. Chem. A* **2004**, *108*, 10640.
(36) Mintova, S.; De Waele, V.; Schmidhammer, U.; Riedle, E.; Bein, T. *Angew. Chem., Int. Ed.* **2003**, *42*, 1611.
(37) Lochbrunner, S.; Wurzer, A. J.; Riedle, E. *J. Phys. Chem. A* **2003**, *107*, 10580.
(38) Elsaesser, T.; Kaiser, W. *Chem. Phys. Lett.* **1986**, *128*, 231.
(39) Laermer, F.; Elsaesser, T.; Kaiser, W. *Chem. Phys. Lett.* **1988**, *148*, 119.
(40) Cohen, B.; Wang, S.; Organero, J. A.; Campo, L. F.; Sanchez, F.; Douhal, A. *J. Phys. Chem. C* **2010**, DOI: 10.1021/jp911730u.
(41) Wiechmann, M.; Port, H.; Frey, W.; Laermer, F.; Elsaesser, T. *J. Phys. Chem.* **1991**, *95*, 1918.
(42) Wiechmann, M.; Port, H.; Laermer, F.; Frey, W.; Elsaesser, T. *Chem. Phys. Lett.* **1990**, *165*, 28.
(43) Zhong, D.; Douhal, A.; Zewail, A. H. *Proc. Natl. Acad. Sci. U. S. A.* **2000**, *97*, 14056.
(44) Douhal, A.; Lahmani, F.; Zewail, A. H. *Chem. Phys.* **1996**, *207*, 477.

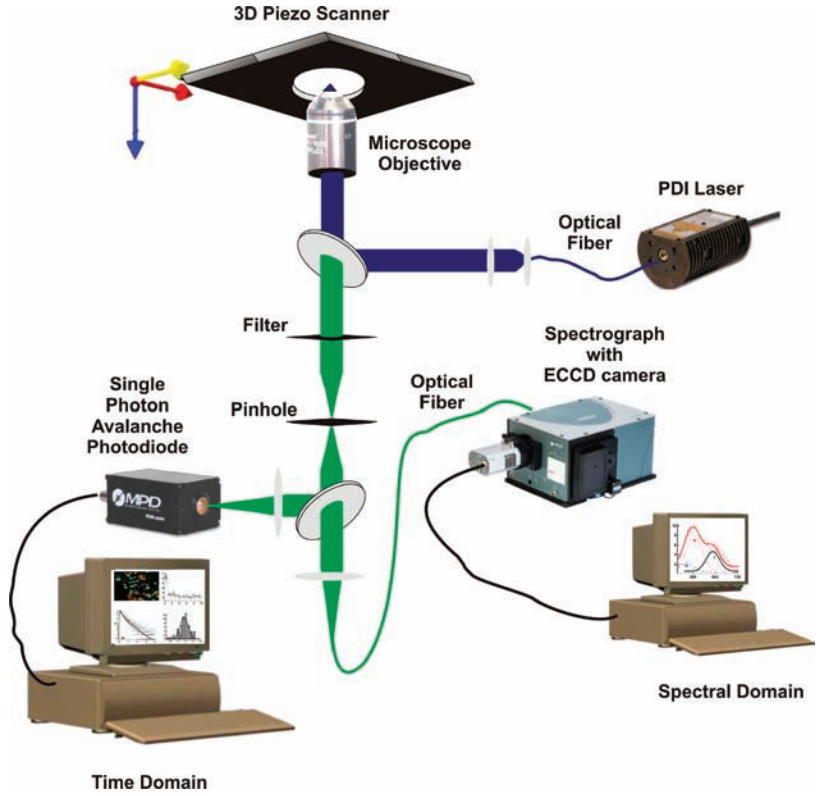

Figure 2. Schematic diagram of the main parts of the time and spectral detections of the experimental SMS system used in this work.

scattered excitation light. Its ground- and excited-state properties are sensitive to various solvent characteristics (polarity, viscosity, and H-bonding), which make it a good candidate for a reporter of changes in the local environment. For example, recently, we reported on the femtosecond excited-state photodynamics of HBTNH2 covalently bonded to silica nanoparticles, MCM-41 and Al-doped MCM-41.[40] We found that the nature of the alumino-silicate host strongly affects the behavior of the guest through strong specific and electrostatic interactions. In (Al)MCM-41 we observe that the excited-state intramolecular proton-transfer reaction is prevented due to the formation in the ground state of phenolate-type anions as a result of the change in the electrostatic properties of the MCM-41 framework. The results reported here provide the experimental basis for improving the design schemes for new nanophotonic devices, catalytic nanoreactors, and dye-based solar cells or to explore the potential application of mesoporous materials in nanomedicine as drug nanocarriers.

Experimental Section

Materials and Methods. We used as guest 2-[5′-*N*-(3-triethoxysilyl)propylurea-2′-hydroxyphenyl]benzothiazole (HBTNH2), a derivative of 2-(2′-hydroxyphenyl)benzothiazole, which shows an excited-state proton-transfer reaction in its enol structure to produce an excited keto or anionic-type species (Figure 1).[49,50] The nature of the materials does not permit straightforward measurement of the fluorescent quantum yield of the studied HBTNH2 structures in the solid state. However, we measured and compared the relative emission quantum yields (in terms of the emission spectrum area related to the normalized one of HBTNH2−(Al)MCM-41) of the covalently bonded dye to MCM-41 and to silica materials in acetonitrile suspensions, for which we used the same value of the diffuse transmittance intensities (in terms of Kubelka−Munk units) at 390 nm (Supporting Information, Figure S1A and S1B). We found that the relative emission quantum yield increases from HBTNH2−silica (0.2), HBTNH2−MCM-41 (0.45), to HBTNH2−(Al)MCM-41 (1). Clearly, the last material, having the emission of the anionic structure (see later) of the guest, is the most fluorescent one.

For the SMS experiments, we have interrogated the emission of between 60 and 100 individual complexes (different crystals, each containing one isolated molecule) of the interacting single dye with MCM-41 and silica nanoparticles (Figures 1 and 2). MCM-41 has unidirectional hexagonal pores with diameters of ∼35 Å.[51] The synthesis of the covalently bonded samples is given in ref 50. The single-molecule samples were prepared by dissolving the solid samples in acetonitrile, sonicating the suspension for 60 min, and diluting it with acetonitrile (spectroscopic grade, 99+%). The diluted solution was then deposited on 100 μm thick quartz support and spin-coated for 2 min. The physical sorption samples were prepared by sonicating the HBTNH2 molecule in a suspension of MCM-41 with random particle size and stirred overnight for better encapsulation. Washed samples were prepared by centrifuging and washing the MCM-41 sample three times with acetonitrille. The particle length of the crystals of MCM-41 ranges between 80 and 200 μm. The size of the guest is significantly smaller ($\sim 10 \times 18 = 180$ Å^2) when compared to the free space provided by the MCM-

(45) Acuña, A. U.; Amat-Guerri, F.; Costela, A.; Douhal, A.; Figuera, J. M.; Florido, F.; Sastre, R. *Chem. Phys. Lett.* **1991**, *187*, 98.
(46) Costela, A.; Amat, F.; Catalan, J.; Douhal, A.; Figuera, J. M.; Munoz, J. M.; Acuña, A. U. *Opt. Commun.* **1987**, *64*, 457.
(47) Douhal, A.; Lahmani, F.; Zehnacker-Rentien, A.; Amat-Guerri, F. *J. Phys. Chem.* **1994**, *98*, 12198.
(48) Catalan, J.; Fabero, F.; Soledad Guijarro, M.; Claramunt, R. M.; Santa Maria, M. D.; Foces-Foces, M. d. l. C.; Hernandez Cano, F.; Elguero, J.; Sastre, R. *J. Am. Chem. Soc.* **1990**, *112*, 747.
(49) Elsaesser, T.; Schmetzer, B. *Chem. Phys. Lett.* **1987**, *140*, 293.
(50) Campo, L. F.; Sanchez, F.; Stefani, V. *J. Photochem. Photobiol., A* **2006**, *178*, 26.
(51) Kresge, C. T.; Leonowicz, M. E.; Roth, W. J.; Vartuli, J. C.; Beck, J. S. *Nature (London, U. K.)* **1992**, *359*, 710.

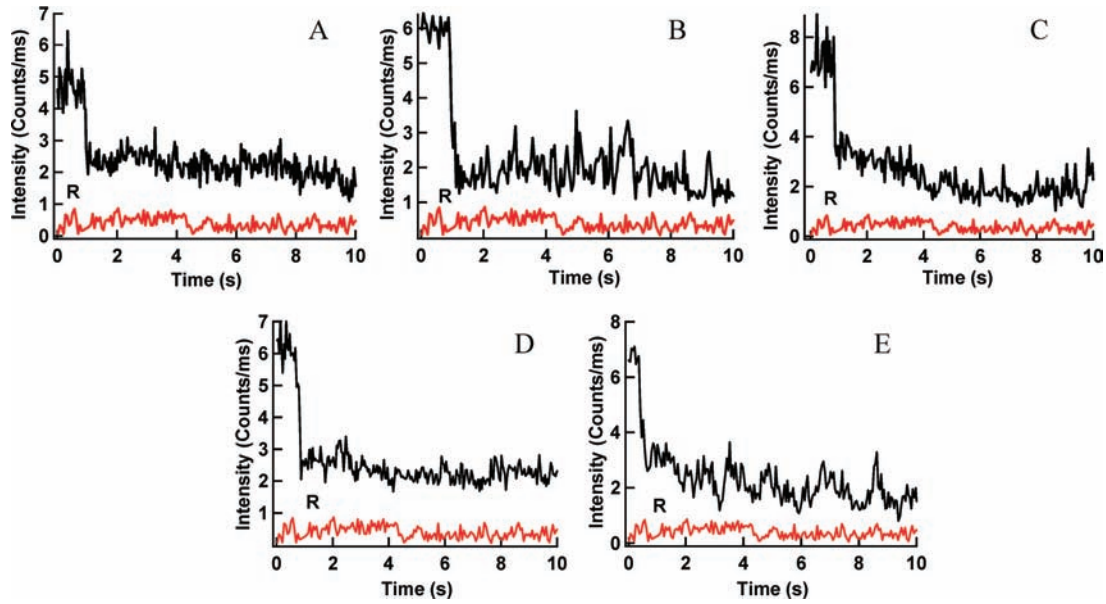

Figure 3. Representative intensity photobleach transients for (A) encapsulated by physical sorption; (B) covalently bonded; (C) encapsulated and washed with acetonitrile HBTNH2/MCM-41 complexes; (D) covalently bonded HBTNH2−silica nanoparticle; and (E) HBTNH2−(Al)MCM-41. R is the signal from the host without the presence of the dye.

41 channel (diameter of ∼4 nm and length between 80 and 200 μm). The particle length of the used silica is about 40−63 μm (silica gel 60, Merck 109385).

Single-Molecule Fluorescence Spectroscopy and Imaging. To produce the photoexcited structures, we used a diode laser (PicoQuant) with an excitation wavelength of 390 nm (40 ps full-width half-maximum), which is within the absorption band corresponding to the first electronically excited state ($S_0 \rightarrow S_1$) of the enol or the phenolate-type anion forms (Supporting Information, Figure S2). The emission signal was collected using a 430 nm long pass filter, thus ensuring response from any of the possible forms is detected. The detection system (Figure 2) consists of an inverse Olympus IX 71 microscope equipped with a water immersion objective (×60 NA1.2, Olympus) and 2D piezo scanner (Physik Instrumente). The emitted light is then focused on a pinhole of 50 μm and later collimated either to the single-photon avalanche photodiode (Micro Photon Devices) for time-resolved measurements or to the entrance of a monochromator (Andor Technology) for spectral observation. Approximately 10% of the beam intensity is reflected by a beam splitter, placed before the major dichroic mirror, to a photodiode unit, which measures the average excitation intensity. The photodiode readout is provided by the control software as a dimensionless number, au, which is converted to laser power units using the calibration curve of absolute power values measured before the entrance pupil of the objective. The excitation power was between 0.02 and 0.1 μW. For the purpose of data acquisition, we used time-correlated single-photon counting (TCSPC) system PicoHarp 300 (PicoQuant). The model we used to fit to the TCSPC decays, included in the closed package (Fluofit, Picoquant), accounts for the scattered excitation light. The quality of the fit was judged by the symmetrical distribution of the residuals around zero. The instrument response function (IRF = 250 ps) was measured from the backscattered excitation light from the quartz support (∼0.1 mm thickness), and the spatial resolution (200 nm) was estimated from the fluorescence image of fluorescently stained latex beads (Molecular Probes, Bangs Laboratories). For the spectrally resolved measurements the emission was collected through a Shamrock SR-303i (Andor Technology) imaging spectrograph and detected by an Andor Newton EMCCD camera (Andor Technology).

Data Analysis. Only fluorescence photobleach time traces that have a sharp transition with the resulting decay signals being monoexponential were taken into account and analyzed to ensure working in the single-molecule regime. This requirement represents a significant challenge due to the low signal level of the single molecule and the background contribution arising from Raman emission, scattered light, and fluorescence from out-of-focus dye molecules. Figure 3 shows representative photobleach traces for the samples used in this work. In our studies we were able to detect contribution from up to three individual molecules within the same mesoporous silica material crystal (Supporting Information, Figure S3). Under our experimental conditions of sample preparation, excitation, and detection, we found that only between 5% and 10% of all the measurements fulfilled the requirements for single-molecule behavior, while the rest of the experiments revealed ensemble-like behavior most likely due to the presence of several HBTNH2 molecules in the nanopores of the selected material or the presence of aggregates/clusters in the studied region. Thus, among hundreds of experiments, between 60 and 100 measurements for individual molecules, interacting with the mesoporous material, were recorded, giving fluorescence decays that were fitted individually using a nonlinear least-squares procedure (NLS) that accounts for scattered light (Fluofit package, Picoquant, Germany). Fluorescence photons emitted by the single chromophore−silica material complex were sampled in time bins of 20 or 30 ms. The quality of the fit was judged by the distribution of the residuals around zero and the value of χ^2, which was between 0.6 and 1.0. Since the total photons detected are between 1000 and 8000 (Supporting Information, Figure S4) for all the experiments, the lifetimes obtained by the NLS are expected to be 5% lower than the ones obtained from the maximum likelihood estimation (MLE).[52] Comparison between the two fitting methods in this range of total photons detected did not yield significant change in the values of the obtained lifetimes, which is in agreement with previous theoretical and experimental observations.[52] The deviation between the two methods was less than 2%, with the MLE giving consistently higher values. This number is within the experimental error of ∼10% and does not affect the analysis of the systems under study. The lifetime distributions were spread over 20 bins. The obtained time constant values correspond to the emission lifetime of an excited single guest and are used to construct a histogram to

(52) Maus, M.; Cotlet, M.; Hofkens, J.; Gensch, T.; De Schryver, F. C.; Schaffer, J.; Seidel, C. A. M. *Anal. Chem.* **2001**, *73*, 2078.

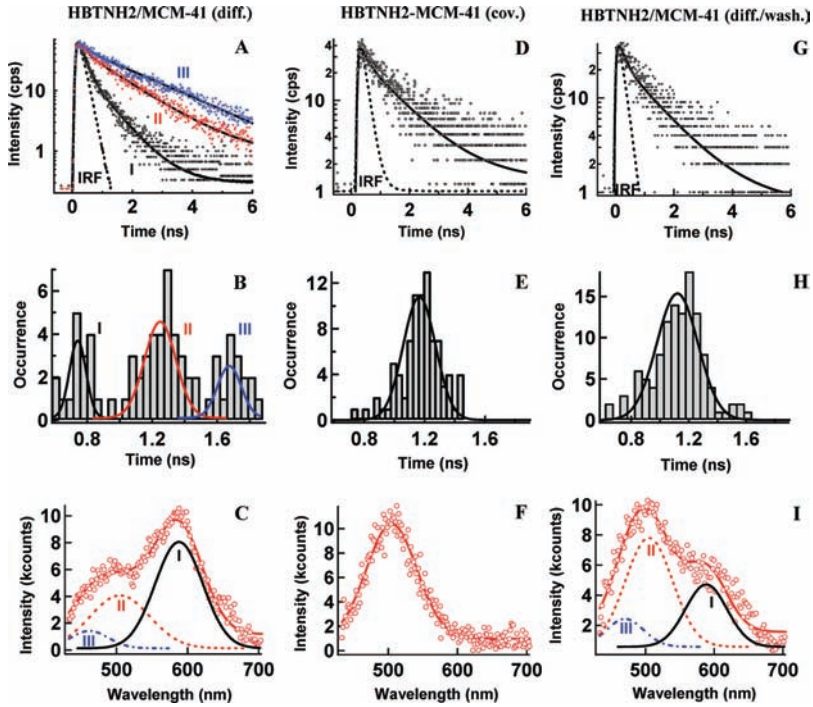

Figure 4. Single molecule spectroscopy results and data analysis of the HBTNH2/unmodified MCM-41 complexes prepared by physical sorption and covalent bonding. Representative decay signals in counts per second (cps) derived from the fluorescence photobleach traces (Figure 3 and Supporting Information, Figures S3) of HBTNH2: (A) encapsulated in MCM-41 by physical sorption; (D) covalently bonded within MCM-41; and (G) encapsulated in MCM-41 by physical sorption and washed with acetomitrile. Solid lines are the nonlinear least-squares monoexponential fits. B, E, and H show the normalized distributions of the lifetimes from the monoexponential fit to the decays of single-molecule MCM-41 complexes prepared by physical sorption, covalently bonded, and by physical sorption and washed with acetonitrile, respectively. The lifetime histograms were fitted by a single (HBTNH2 covalently bonded to MCM-41 or physisorbed and washed) or three separate Gaussian functions (complexes prepared by physical sorption). The parameters for the fit are given in Table 1. C, F, and I represent the average spectrum of HBTNH2 physisorbed by MCM-41, covalently bonded within MCM-41, and physisorbed by MCM-41 and washed with acetonitrile, respectively. The average spectra were smoothed by a five-point average and fit to a single or three Gaussian distributions (full line). The parameters of the fit are given in Table 2. The Roman numerals I, II, and III refer to the excited-state population, as discussed in the text.

Table 1. Values of the Sample Emission Lifetimes (τ_i), Normalized (to 100) Relative Contributions (a_i), and the Full-Width at Half-Maximum of Lifetimes Distribution (w_i) from the Gaussian Fit

sample	τ_1 [ns]	a_1 [%]	w_1 [ns]	τ_2 [ns]	a_2 [%]	w_2 [ns]	τ_3 [ns]	a_3 [%]	w_3 [ns]
HBTNH2−silica	0.70	100	0.24						
HBTNH2−silica (DBU)	0.70	100	0.28						
HBTNH2−(Al)MCM-41	0.88	100	0.11						
HBTNH2−MCM-41				1.17	100	0.23			
HBTNH2/MCM-41	0.74	20	0.18	1.25	50	0.32	1.67	30	0.23
HBTNH2/MCM-41 (washed)				1.14	100	0.44			

get information on the distribution of a single behavior along 60−100 samples.

The spectral response of the single-molecule−silica material complexes was reconstructed by averaging 60−100 individual spectra collected at 3 s integration time. The intensity of the signals was not sufficient to perform simultaneous or consecutive measurement in the time and spectral domains. In order to ensure a single-molecule regime in the spectral collection, during the time domain experiment for each sample, the intensity of ∼100 molecular complexes was analyzed. This yielded a threshold for the image intensity of single molecules. All the spectra were collected for complexes (images) below the derived intensity threshold.

Results and Discussion

We first examined the emission of single 2-[5′-N-(3-triethoxysilyl)propylurea-2′-hydroxyphenyl]benzothiazole (HBTNH2)/mesoporous silica material (MCM-41) complexes prepared by physical sorption using the SMS technique (Figures 1 and 2). The single-lifetime histogram shows a multimodal behavior (Figure 4A,B) with three distinctive Gaussian distributions assigned to different excited-state populations: I, centered at 0.74 ns (width, $w = 0.18$ ns), II, on 1.25 ns ($w = 0.32$ ns), and III on 1.67 ns ($w = 0.23$ ns) (Figure 4B and Table 1). These subpopulations reflect three different modes of interaction of the dye with the MCM-41 framework. This multimodal distribution is also seen in the spectral response of the single HBTNH2/MCM-41 complexes collected in a separate experiment from the data for the lifetime histogram (Figure 4C). A more precise deconvolution of the combined emission spectrum of 72 single-molecule spectra suggests three contributing bands with the major one positioned at 588 nm (56% to the overall emission spectrum). The other two bands are positioned at 462 nm (11%) and 505 nm (33%) (Table 2). The above result is consistent with the existence of three sites of sorption in MCM-41. Unfortunately, due to the low fluorescence intensity and the irreversible photobleaching (even at the lowest laser power to detect a signal from the sample during the experiment), a simultaneous or consecutive detection of the fluorescence time

Table 2. Values of the Normalized (to 100) Relative Contribution (a_i) of Each Spectral Band and the Wavelength at the Intensity Maximum (P_i) of the Emission Band and of Its Full-Width at Half-Maximum (w_i) of Intensity from the Gaussian Fit

sample	P_1 [nm]	a_1 [%]	w_1 [nm]	P_2 [nm]	a_2 [%]	w_2 [nm]	P_3 [nm]	a_3 [%]	w_3 [nm]
HBTNH2−silica							588	100	89
HBTNH2−silica (DBU)	480	9	75				605	91	85
HBTNH2−(Al)MCM-41							583	100	64
HBTNH2−MCM-41 (cov.)				505	100	93			
HBTNH2-MCM-41 (diff.)	462	11	82	505[a]	33	110	588[a]	56	87
HBTNH2−MCM-41 (diff., washed)	470	14	82	505[a]	55	89	588[a]	31	85

[a] Fixed values following the model presented in the text.

traces and the spectrum of the same single HBTNH2/MCM-41 complex cannot be performed in order to make a multiparameter fluorescence analysis. Multiparameter detection and analysis of single-molecule experiments have provided information regarding the distribution of multiple populations within chemical and biological systems.[53,54]

Next, we restricted the number of possible location sites by covalently bonding HBTNH2 to the inner surface of MCM-41 (Figure 1D). The single-lifetime histogram (89 experiments) reveals a single distribution, fitted with a Gaussian function, centered at 1.17 ns with $w = 0.23$ ns (Figure 4D,E). This single distribution is further reflected by the behavior of the average emission spectrum reconstructed from 86 single experiments (Figure 4F), fitted to a single Gaussian function, and centered at 505 nm ($w = 93$ nm; $\sim$3250 cm^{-1}). The spectral broadening and the relatively narrow and symmetric distribution of the single-molecule lifetimes suggest ultrafast conformational changes in the single photoproduced keto structure. The later arises from the excitation of the enol form bonded to MCM-41. Femtosecond spectroscopy has probed the conformational changes in comparable dyes (ensemble average regime), confined in chemical and biological nanocavities, and the observed ultrafast dynamics has been explained in terms of confinement effect on the barriers of the potential energy surface.[34,43] SMS was applied to characterize the interaction between a dye molecule and polymer matrix.[11,12,55,56] The observed broadening in the normalized lifetime distribution was correlated with the influence of the local microenvironment.[11,56] For the complexes prepared by physical sorption (Figure 4B), the intermediate distribution in the lifetime histogram ($\sim$50% of the overall events (population II)) shows a normalized lifetime (1.25 ns) comparable to the one found for the chromophore covalently bonded into the nanochannel (1.17 ns) (Figure 4E). This result suggests that the related emitting single species in the noncovalently bonded complex is embedded within MCM-41, having comparable interaction to that of the bonded single molecule. Thus, the largest population of single molecules encapsulated within MCM-41 feels the specific properties of the internal walls of the nanopores, having OH groups favoring the formation of H-bonds with the encapsulated dye. Since the large internal surface has more hydroxylic groups than the external one, it facilitates the encapsulation and stabilization of molecules that favor H-bond formation. The width of the normalized lifetime distribution for the covalently bonded complexes (0.23 ns) is about 30% narrower than the one for the encapsulated population (II), 0.32 ns. This difference suggests larger variations in the effect of the local environment on the encapsulated diffusing molecule, allocating more freedom in conformational changes in the rings' relative position in the photoformed keto structure.

To further characterize the sites of interaction of noncovalently bonded HBTNH2 to MCM-41, the complexes prepared by physical sorption were studied after a washing procedure using acetonitrile, in order to decrease the population of the weakly interacting molecules with the host external surface. Analysis of the single-molecule emission behavior reveals a dramatic change in both the averaged spectra and the lifetime histogram (Figure 4G−I). The latter fits to a single Gaussian distribution, opposed to the three distinct ones seen in the case of unwashed samples (Figure 4H,B, respectively). The fit is centered at 1.14 ns with a distribution width, w, of 0.44 ns. The lifetime is close to that found for the guest covalently bonded to the inner surface (1.17 ns) or encapsulated within the MCM-41 nanochannel (1.25 ns), while the width is almost twice that found for the covalently bonded molecule ($w = 0.23$ ns) and 30% higher compared to a single distribution (I, II, or III) of unwashed encapsulated complexes. This is an indication that there still exists a small population of HBTNH2, weakly bonded to the outer surface of the MCM-41 crystal. This is further confirmed by the spectral behavior, where we again find three bands but with changed contributions with the maximum in intensity at 505 nm (Figure 4I).

Single molecules adsorbed on the outer surface of MCM-41 are not under the influence of the confinement effect of the nanopores but will reflect the interactions with the O−Si−O framework. We have investigated single HBTNH2 molecules covalently bonded to silica particle surface (Figure 1E). Notice that the situation mimics that of the dye attached to the outer surface of the MCM-41 crystal. Therefore, we recorded and analyzed 94 fluorescence traces (Figure 3D and Figure S3) and constructed the lifetime histogram (Figure 5A,B). We observed a single Gaussian distribution centered at 0.70 ns with $w = 0.24$ ns. Both values are consistent with the shortest lifetime and width (0.74 and 0.18 ns, respectively) of population I found for the complexes prepared by physical sorption discussed above (Figure 4B). The spectral behavior of 73 single-molecule silica complexes shows a single band centered at 588 nm with a width of 89 nm ($\sim$2750 cm^{-1}) (Figure 5C). To characterize the structure and the type of interactions with the nanochannel that are behind this single-molecule emission spectrum, we have added 1,8-diazabicyclo[5.4.0]undec-7-ene (DBU), a strong organic base, in order to form at the ground state the anion (phenolate type) of HBTNH2 covalently bonded to silica (Supporting Information, Figure S5). The results show that the emitting species in both the monitored single-molecule silica complexes and the one giving a lifetime of 0.70 ns in the unwashed HBTNH2/MCM-41 (population I) (Figure 4A−C)

(53) Eggeling, C.; Berger, S.; Brand, L.; Fries, J. R.; Schaffer, J.; Volkmer, A.; Seidel, C. A. M. *J. Biotechnol.* **2001**, *86*, 163.
(54) Rothwell, P. J.; Berger, S.; Kensch, O.; Felekyan, S.; Antonik, M.; Wohrl, B. M.; Restle, T.; Goody, R. S.; Seidel, C. A. M. *Proc. Natl. Acad. Sci. U. S. A.* **2003**, *100*, 1655.
(55) Vallee, R. A. L.; Cotlet, M.; Van der Auweraer, M.; Hofkens, J.; Muellen, K.; De Schryver, F. C. *J. Am. Chem. Soc.* **2004**, *126*, 2296.
(56) Vallee, R. A. L.; Van Der Auweraer, M.; De Schryver, F. C.; Beljonne, D.; Orrit, M. *ChemPhysChem* **2005**, *6*, 81.

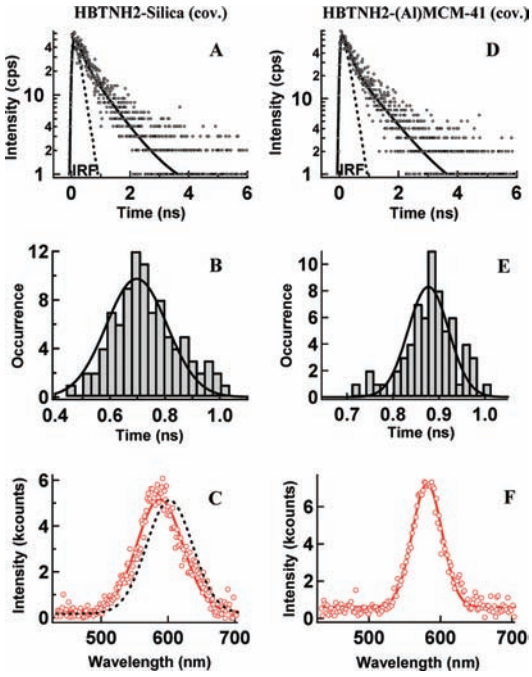

Figure 5. Single-molecule spectroscopy results and data analysis of the HBTNH2 covalently bonded complexes with silica nanoparticle and Al-doped MCM-41. Representative decay signals in counts per second (cps) derived from the photobleach traces (Figure 3 and Supporting Information, Figure S3) of HBTNH2 covalently bonded to (A) silica and (D) (Al)MCM41, along with the nonlinear least-squares monoexponential fits (solid lines). B and E are the distributions of the lifetimes from the monoexponential fit to the decays of single-molecule silica and (Al)MCM-41 complexes, respectively. The lifetime distributions were fitted by a single Gaussian function (Table 1). C and F represent the average emission spectrum of a single HBTNH2 covalently bonded to a silica nanoparticle and (Al)MCM-41 nanochannels, respectively. The average spectra were smoothed by a 5-point average and fit to a single Gaussian (full line). The parameters of the fit are given in Table 2. The dashed line in part C represents the Gaussian fit to the main contributing band in the average spectrum of single HBTNH2−silica complexes in the presence of the strong base 1,8-diazabicyclo[5.4.0]undec-7-ene (DBU) (see text and Supporting Information, Figure S5).

are from an excited anion generated by direct excitation of its structure at the ground state (Supporting Information, Figure S2). In both cases, strong electrostatic interactions are behind the spectral and time domain behavior.

We therefore used the spectral features, found for single molecules covalently bonded to the silica surface (Figure 5C) and to the inside of the MCM41 nanochannel (Figure 4F), to fit the averaged emission spectrum of the single-molecule MCM-41 complexes, formed by physical sorption (Figure 4C,I). In agreement with the three populations seen in the lifetime histogram, we find three bands in the averaged spectrum of the unwashed MCM-41 complexes (Table 2). We assign the band at 505 nm to a keto form (population II) encapsulated inside the MCM41 framework, similar to the covalently bonded HBTNH2 into MCM41, whereas the 588 nm band is assigned to phenolate-type anion (population I) attached to the outer surface of the mesoporous material, similar to the HBTNH2 covalently bonded to silica (Figure 1F). We also find a band centered around 462 nm, which we correlate to the Gaussian distribution centered at 1.67 ns in the lifetime histogram. This band is present also in the ensemble average steady-state emission spectra of the unwashed samples in the acetonitrile suspension, prepared by physical sorption, but disappears in the ensemble average emission spectra of the washed HBTNH2/MCM41 (Supporting Information, Figure S6A). The band position is close to the one found for the open enol form of HBT (430 nm) having formed H-bonds with solvent molecules or OH groups of the mesoporous silicate framework.[40] Furthermore, upon excitation at 330 nm (the intensity maximum of absorption of the open enol form) of the unwashed samples in acetonitrile suspension, the ensemble average emission spectrum shows an increase in the emission band centered at 430 nm in comparison to the one collected after excitation at 390 nm, where the open enol structure has a relatively lower extinction coefficient (Supporting Information, Figure S6B). Thus, we suggest that population III is arising from the enol form attached through H-bonds to the gate of the nanochannels. Similar analysis was performed for the "washed" dye/MCM-41 complexes. The band centered at 505 nm increases 1.6 times its contribution, while the one at 588 nm decreases by the same extent. This observation further supports the explanation, described earlier, where the 588 nm band and the related 0.74 ns lifetime were assigned to a population of excited anion found at the surface of MCM-41, while the band at 505 nm and lifetime of 1.25 ns were assigned to an encapsulated population of excited keto-type structure formed after intramolecular photoinduced proton transfer.

When Si^{4+} ions are replaced by Al^{3+} ones in the MCM-41 framework, the host becomes more alkaline (Lewis basicity definition) due to the resulting formation of negative charges, neutralized by Na^+ counterions, within the nanopores.[57] The created electrostatic environment may lead to a ground-state deprotonation of the HBTNH2, producing a phenolate-anion type. Such a process is observed in the diffuse reflectance spectra of HBTNH2−(Al)MCM-41 complexes (Supporting Information, Figure S2). Thus, we have monitored the single-molecule emission of the HBTNH2-anion covalently linked inside the (Al)MCM-41 nanochannel, where ~1% of the Si^{4+} atoms were replaced by Al^{3+} ones (Figure 5D−F). The obtained single-lifetime histogram shows a single distribution with a Gaussian shape centered at 0.88 ns with $w = 0.11$ ns. These values significantly differ from those corresponding to the single molecule (keto type) in the unmodified MCM-41, where the Gaussian fit is centered at 1.17 ($w = 0.23$) ns. The Gaussian fit to the averaged spectra of the single-molecule complexes (HBTNH2−(Al)MCM-41) reveals a single band centered at 583 nm with a width of 64 nm (~1480 cm^{-1}) (Figure 5F). It is much narrower than the spectrum of the unmodified MCM-41 (~3250 cm^{-1}) and silica particle (~2750 cm^{-1}) samples. This difference, along with the narrower lifetime distribution ($w = 0.23$ ns), is a clear indication of a stronger confinement of the local nanoenvironment around the single anion within (Al)MCM-41. The replacement of Si by Al atoms changes the electronic density distribution within the framework of MCM-41 and affects the properties of HBTNH2. Thus, the electrostatic orbitals interaction of the guest and host is affected in such manner that the resulting emission comes from a much narrower density of states of the single chromophore.

Conclusions

In conclusion, by mapping the individual distribution of a chromophore interacting with silica-based nanopores and nanoparticles, we have shown that depending on the mode of preparation, the behavior of the formed complex exhibits a large change in emission time and spectral domain. Furthermore, the

(57) Corma, A. *Chem. Rev. (Washington, DC, U. S.)* **1995**, *95*, 559.

results show the significant effect of the electrostatic forces on the nanoconfinement of the anionic-type guest with the nanopores. As a result, the efficiency of a mesoporous silica-based nanophotonic device or a drug-delivery nanocarrier should be dependent on the chemical doping of the host and on the distribution of the guest (fluorophore or drug) in its framework.

Acknowledgment. This work was supported by the JCCM and MICINN through projects PCI08-5868, UNCM05-23-025, MAT2008-01609, and Consolider-Ingenio 2010 (MULTICAT, CDS2009-00050), respectively. B.C. thanks the MICINN for the Ramon y Cajal contract. We thank Dr. L. F. Campo for her help in the synthesis of the materials.

Supporting Information Available: Additional information about the sample preparation, steady-state properties, and photobleach traces of the samples. This material is available free of charge via the Internet at http://pubs.acs.org.

JA100771J